Available online at www.sciencedirect.com
ScienceDirect
Polymer 48 (2007) 5024–5029
polymer
www.elsevier.com/locate/polymer

Dendrimer-encapsulated gold nanoparticles as building blocks for multilayer microshells

Olga V. Lebedeva [a], Byoung-Suhk Kim [b], Franziska Gröhn [c], Olga I. Vinogradova [d,*]

[a] N.S. Enikolopov Institute of Synthetic Polymer Materials, Russian Academy of Sciences, 117393 Moscow, Russia
[b] Sogang University, 1 Shinsu-Dong, Mapo-Gu, Seoul 121-742, South Korea
[c] Max Planck Institute for Polymer Research, Ackermannweg 10, Mainz 55128, Germany
[d] A.N. Frumkin Institute of Physical Chemistry and Electrochemistry, Russian Academy of Sciences, 119991 Moscow, Russia

Received 5 May 2007; received in revised form 13 June 2007; accepted 14 June 2007
Available online 22 June 2007

Abstract

We report the effect of gold nanoparticles encapsulated into the shell-forming PAMAM dendrimers on the assembly and properties of multilayer microshells. We demonstrate that the PAMAM-encapsulated gold nanoparticles change dramatically the optical spectroscopic properties of microcapsule dispersions, without significantly affecting the stiffness of microcapsules. Our results indicate that the use of dendrimer-protected nanoparticles as building blocks opens numerous possibilities to vary the composition and diverse properties of microshells without changing their stiffness.

Keywords: Microshells; Dendrimers; Nanoparticles

1. Introduction

In recent years polyelectrolyte multilayer microcapsules [1] became extremely important and have found numerous applications in various fields of science and technology. They allow encapsulation of various materials, which are normally loaded into the capsule interior and dramatically change osmotic equilibria [2–4], and, as a result, a response of capsules to mechanical signals [5–8]. Here we deal with microcapsules containing cationic poly(amidoamine) dendrimers (PAMAM) as building blocks. These structures potentially allow two types of encapsulation: one in the dendrimers localized in the multilayer shells, and another in the microcapsule interiors resulting in a dual delivery and/or release system. To deposit nanoparticles into capsule shells we do not use standard approaches that take advantage of using inorganic particles as building blocks for the shell formation [9], or an in situ synthesis in multilayer shells [10,11]. Instead, we employ a recently discovered the ability of dendrimers to form organic–inorganic composites [12–19], and synthesize nanoparticles into the PAMAM, which is used then as building blocks for the multilayer shell assembly.

As an initial application of our approach, here we decided to limit ourselves with PAMAM-encapsulated gold nanoparticles, widely used and the most stable metal nanoparticles. The use of gold nanoparticles opens fascinating possibilities in various fields especially due to size-related electronic and optical properties (quantum size effects). Their promises are in the bottom–up approach of nanotechnology, and they are expected to be the key materials and building blocks in the 21st century [20]. The gold nanoparticles and their assemblies were already used as various sensors [21], for catalytic purpose [18,22–24], in biological imaging [25], and as building blocks for the preparation of thin supported films [26,27], which provide a new development of thin conducting or catalytic films [28], sensors, biotechnology [20] and more.

* Corresponding author.
E-mail address: oivinograd@yahoo.com (O.I. Vinogradova).

0032-3861/$ - see front matter © 2007 Elsevier Ltd. All rights reserved.
doi:10.1016/j.polymer.2007.06.036

Despite growing interest in the assembly of various types of multifunctional nanoparticle-based [29–32] and dendrimer-based [33–36] microcapsules and other materials, we are unaware of recent attempts to make microcapsules containing nanoparticles inside shell-forming dendrimers. Here we try to compensate this lack of experimental information. We prepare a new type of microcapsules using PAMAM-encapsulated gold nanoparticles, and demonstrate a remarkable difference in several parameters of capsule dispersions from those typical for PAMAM-based capsules prepared without being loaded by gold. Since the stability and mechanical parameters of multilayer shells are one of the most important characteristics of these systems in our paper we try to focus not only on the preparation and characterization of dendrimer-based microcapsules loaded with gold nanoparticles, but also on their mechanical characteristics. We demonstrate that the remarkable consequence of the encapsulation of gold nanoparticles into dendrimers is that this practically does not influence the stiffness of the multilayer shell. This opens enormous possibility to vary properties and functionalities of shells without changing their mechanical characteristics.

2. Experimental

2.1. Materials

Polysterene sulfonate (PSS, $M_w \sim 1\,000\,000$), auric acid $HAuCl_4$, and the fluorescent dye fluorescein isothiocyanate (FITC) were purchased from Sigma–Aldrich Chemie GmbH, Germany. Sodium borohydride ($NaBH_4$) was purchased from Fluka. Hydrochloric acid (HCl) and sodium chloride (NaCl) were purchased from Riedel-de Haën, Germany. Poly(amidoamine) dendrimers of generation 9 (G9 PAMAM) were supplied by Dendritech, Inc. (Michigan Molecular Institute) [37]. All chemicals were of analytical purity or higher quality and were used without further purification. Water used for all experiments was purified by a commercial Milli-Q Gradient A10 system containing ion exchange and charcoal stages, and had a resistivity of 18.2 MΩ/cm. The pH was measured using pH meter (InoLab, Germany) with the accuracy of ±0.5.

Suspensions of monodispersed weakly cross-linked melamine formaldehyde particles (MF particles) with a radius of $r_0 = 2.0 \pm 0.1$ μm were purchased from Microparticles GmbH (Berlin, Germany). Glass bottom dishes (0.17 mm/∅ 30 mm) with optical quality surfaces were obtained from World Precision Instruments Inc. (USA). Glass spheres (radius 20 ± 1 μm) were purchased from Duke Sci. Co., California.

2.2. Methods

2.2.1. Synthesis and characterization of Au nanoparticle-loaded G9 PAMAM dendrimers

The synthesis and characterization of the G9 PAMAM dendrimer encapsulated with Au nanoparticles (G9 Au-PAMAM) have been described previously [18]. Briefly, aqueous solutions of G9 PAMAM dendrimers ranging from 0.1 to 1.0% mass fraction were prepared by diluting concentrated dendrimer/methanol solutions (dendrimer mass fraction of 20–25%) with deionized water. Dilute aqueous solutions of G9 PAMAM dendrimers were mixed with aqueous solutions of $HAuCl_4$ at controlled stoichiometries. After stirring these solutions for 1 h, sodium borohydride in basic aqueous solution (0.025–0.5 M sodium hydroxide) was added. The light yellow dendrimer/$HAuCl_4$ solutions immediately turned deep red, indicating the formation of colloidal gold. The brown or red color of the solutions and UV–vis spectra are typical of gold colloids. The presence of gold nanoparticles inside the dendrimers was previously confirmed by transmission electron microscopy (TEM) and small-angle X-ray scattering (SAXS). TEM on the dendrimer–gold particles was performed after staining the dendrimer and it is evident that the colloid particles are formed inside the dendrimer. The sizes estimated for the dendrimer and gold are 13 and 4 nm, respectively. This value corresponds to previous reports of the size of the unmodified PAMAM dendrimers within the experimental error [38]. SANS results for the dendrimer–gold hybrid particles also show that the radius of gyration obtained from Guinier extrapolation is 5.1 ± 0.1 nm. The result indicates that the hybrid particles also do not form larger aggregates in solution. The detailed descriptions are written in the previously reported paper [18].

2.2.2. Capsule preparation

The PSS/PAMAM and PSS/Au-PAMAM capsules were prepared similar to the method described in Ref. [33] and as schematically shown in Fig. 1. The positively charged MF particles (50 μL of 10 wt% water dispersion) as a template were incubated with 1 mL of PSS solution (1 mg/mL containing 0.5 mol/L NaCl, pH 6) at room temperature for 10 min, followed by three centrifugation/rinsing cycles, and finally dispersed in water. A 1 mL portion of a PAMAM or Au-PAMAM solution (1 mg/mL, pH 4) was then added to the particle dispersion. After 20 min given for adsorption three centrifugation/wash cycles were performed (as above). The PSS and

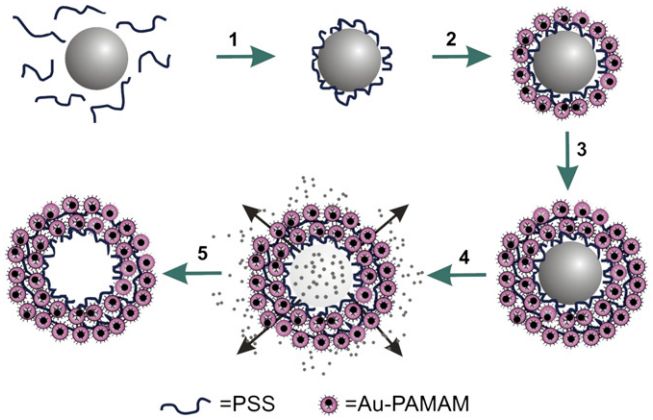

Fig. 1. LbL assembly of PSS/Au-PAMAM microcapsules. 1 – PSS adsorption; 2 – Au-PAMAM adsorption; 3 – repeat of the steps 1 and 2; 4 and 5 – template decomposition.

PAMAM (or Au-PAMAM) adsorption steps were repeated four times each to build multilayers on the MF particles. Each adsorption was followed by washing out excess polymer and salt. The microcapsules referred to below as $(PSS/PAMAM)_4$ and $(PSS/Au\text{-}PAMAM)_4$ capsules were obtained by dissolving the MF template in HCl at pH 1.2–1.6 and washing with water three times as described before. For the preparation of the microcapsules referred to below as $(PSS/PAMAM)_4$/PSS and $(PSS/Au\text{-}PAMAM)_4$/PSS additional layer of PSS was absorbed before dissolving the MF template.

UV–vis spectra of $(PSS/PAMAM)_4$ and $(PSS/Au\text{-}PAMAM)_4$ microcapsule suspensions were obtained on a Perkin–Elmer Lambda 9 spectrometer in the wavelength range 300–800 nm.

2.2.3. Microscopy

Confocal laser scanning microscopy images were taken with a commercial confocal microscope unit FV300 (Olympus, Japan) used in combination with an inverted fluorescence microscope Olympus IX70. A high resolution (60×) bright (NA = 1.45) oil immersion objective was used. The drop of suspension of capsules was applied to a glass bottom dish with subsequent addition of water. High resolution and contrast of the confocal images were achieved by the use of low molecular fluorescent dye FITC added to the capsule solution at a concentration of $\sim 10^{-6}$ mol/L. The excitation wavelength was $\lambda = 488$ nm.

For scanning electron microscopy (SEM) analysis a drop of suspension of capsules was applied to a silicon wafer with sequential drying at room temperature for several hours [39]. The measurements were performed using a Gemini Leo (Zeiss) 1530 instrument operating at a working distance of 2 mm and an acceleration voltage of 0.5 kV. Since the samples were not covered with a gold layer before inspection, this low acceleration voltage was applied in order to avoid charging of the sample. The images were recorded using the InLens Detector.

For TEM examination one drop of sample solution was applied to a carbon coated copper TEM grid. Excess solution was blotted off with a piece of filter paper. The remaining sample solution on the carbon film was allowed to dry at room temperature before examined by TEM. Inspection of the dry capsules was performed in a LEO 912 transmission electron microscope at an acceleration voltage of 120 kV. Images were taken on a 1k Proscan CCD Camera.

2.2.4. Force measurements

The experimental set-up was described before [40–42]. Briefly, load (force) vs deformation curves were measured with the molecular force probe device (MFP) 1D (Asylum Co., Santa Barbara, USA), which has a nanopositioning sensor that corrects hysteresis and creep of the piezo translator. For the force measurements we used V-shaped cantilevers (MikroMasch, Estonia, spring constants $k \approx 3.0$ N/m). Exact spring constant of the cantilever was estimated from the resonant frequency calibration plot. Briefly, MikroMasch cantilevers have six parameters in the specification, namely, three values for the typical resonant frequency and, respectively, three spring constants, calculated from their geometric (length, width, height) and physical (density, resonant frequency) parameters [43]. These values (resonant frequencies and spring constants) were entered in the plot and line regression was made in order to fit data points. Then the resonant frequency of the cantilever was measured and its spring constant was determined from the calibration plot. The spring constants determined by this method were compared with spring constants determined by the method of added mass [44] and good agreement was found. Glass spheres were glued onto the apex of cantilevers with epoxy glue (UHU Plus, Germany). The capsule deformation experiment has been described before [42]. Here we performed the dynamic measurements at intervals of piezo translator speed from 0.2 to 20 μm/s. The result of the measurement represents the deflection Δ vs the position of the piezo translator at a single approach. The force F was determined from the cantilever deflection, $F = k\Delta$. As before, we assume that zero separation is at the point of the first measurable force [6]. Then the deformation is calculated as the difference between the position of the piezo translator and the cantilever deflection. The diameter of the capsule was determined optically with an accuracy of 0.2 μm and from the AFM load vs deformation curves (like in Ref. [6]). The relative deformation ε of the capsule was then calculated as $\varepsilon = 1 - H/(2r_0)$, where H is the minimum sphere/substrate separation [6,41]. To get reliable results we have performed several series of force measurements. Every series included at least 10 experiments. Then the average of all force vs deformation curves was calculated.

3. Results and discussion

3.1. General observations

Fig. 2 (top) shows suspensions of MF particles (a), $(PSS/PAMAM)_4$ microcapsules (b) and $(PSS/Au\text{-}PAMAM)_4$ capsules (c). As one can see, the suspension of $(PSS/PAMAM)_4$ capsules is colorless and transparent while the suspension of $(PSS/Au\text{-}PAMAM)_4$ capsules is dark red, like the color of Au-PAMAM solution used for the capsule preparation. The capsules made using Au-PAMAM precipitate much faster as compared with capsules without gold nanoparticles. From the UV–vis spectra of $(PSS/PAMAM)_4$ and $(PSS/Au\text{-}PAMAM)_4$ microcapsule suspensions (Fig. 2, bottom) one could see that Au-containing microcapsules show a surface plasmon band in the visible region around 520 nm, indicating the presence of Au nanoparticles (a rough estimate leads to a particle size below ca. 4–5 nm). This is well consistent with the TEM data. The shape of the obtained capsules and their average diameters were monitored by confocal laser scanning microscopy. Typical image of $(PSS/Au\text{-}PAMAM)_4$ capsules is shown in Fig. 3. The absolute majority of them (>90%) have ideal spherical shape. The $(PSS/PAMAM)_4$, $(PSS/PAMAM)_4$/PSS and $(PSS/Au\text{-}PAMAM)_4$/PSS capsules have given similar confocal images. SEM and TEM images of dried capsules (Fig. 4) were also taken in order to observe and confirm the formation of the capsules.

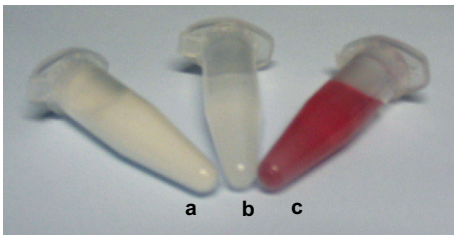

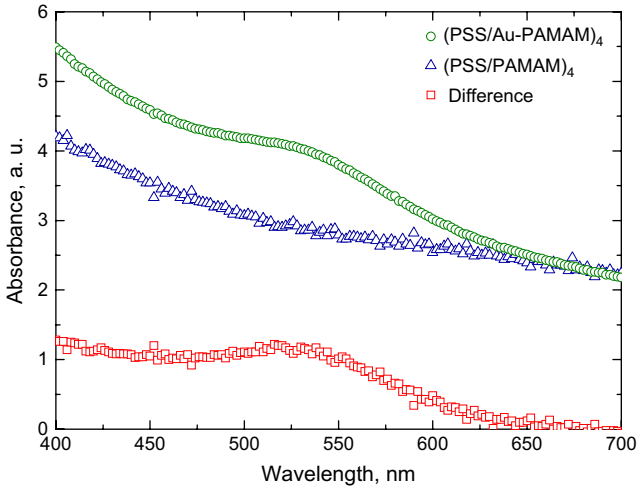

Fig. 2. Top: suspensions of MF particles (a), $(PSS/PAMAM)_4$ microcapsules (b) and $(PSS/Au\text{-}PAMAM)_4$ capsules (c). Bottom: UV–vis spectra of $(PSS/PAMAM)_4$ and $(PSS/Au\text{-}PAMAM)_4$ microcapsule suspensions and the difference.

3.2. Structure and morphology of the capsules

To investigate the multilayer shell structure and morphology, we have taken and analyzed SEM and TEM images of dried capsules at higher magnification (Fig. 4c and d). The surface morphology of capsules (Fig. 4a and c) shows the folds with sharp edges similar to the majority of microcapsules studied before [45,46]. The surface of the capsules looks rough, but it is not porous. TEM analysis has shown that gold nanoparticles are included in the shell of $(PSS/Au\text{-}PAMAM)_4$ microcapsules and that these nanoparticles are well separated (Fig. 4d). These results demonstrate that gold nanoparticle-loaded PAMAM dendrimer can be successfully used as a building block for the formation of multilayer microcapsules.

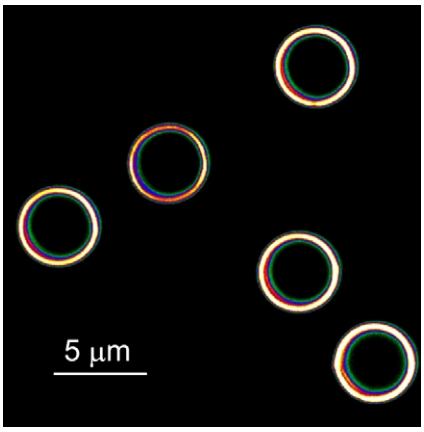

Fig. 3. The confocal image of $(PSS/Au\text{-}PAMAM)_4$ microcapsules.

3.3. Deformation profiles

Fig. 5 shows the average force vs deformation profiles for $(PSS/PAMAM)_4$, $(PSS/PAMAM)_4/PSS$, $(PSS/Au\text{-}PAMAM)_4$, and $(PSS/Au\text{-}PAMAM)_4/PSS$ microcapsules. One can see that capsules containing gold nanoparticles in their shells are somewhat stiffer than their gold-free analogues, but the

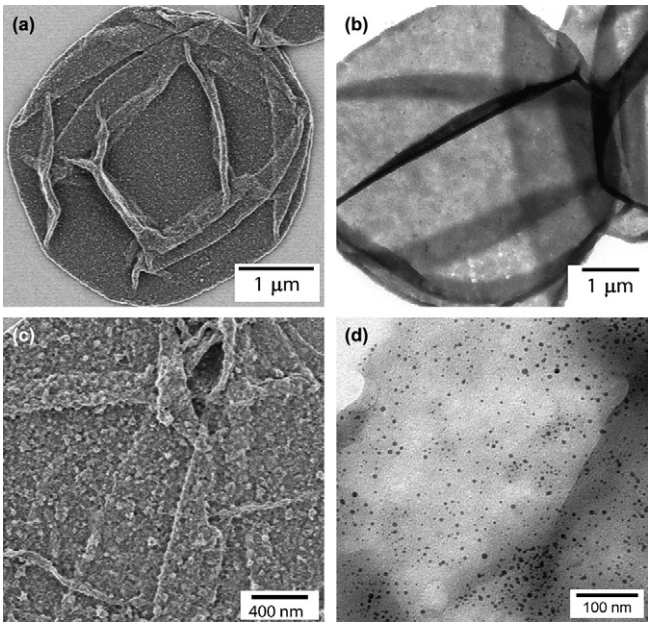

Fig. 4. SEM (a and c) and TEM (b and d) images of $(PSS/Au\text{-}PAMAM)_4$ microcapsules.

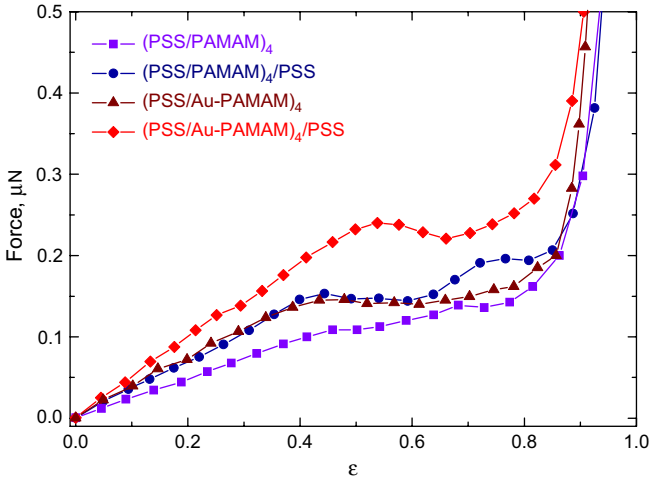

Fig. 5. The average force–deformation curves measured for $(PSS/PAMAM)_4$, $(PSS/PAMAM)_4/PSS$, $(PSS/Au\text{-}PAMAM)_4$ and $(PSS/Au\text{-}PAMAM)_4/PSS$ capsules. For all curves only every 15th point is shown.

increase in the stiffness is not significant. It has previously been concluded [31] that the presence of nanoparticles in the multilayers should always dramatically increase the stiffness. Also note that PAMAM dendrimers are rather soft and can be easily deformed, so that being deposited to the oppositely charged solid surface they compress to the ellipsoidal shape (with the height of about 5–6 nm for the PAMAM of the diameter used here) [47]. Therefore, the presence of a metal nanoparticle inside a dendrimer molecule should change the stiffness of dendrimers significantly. However, our results clearly show that this is not so for multilayer shells made of PAMAM-encapsulated gold. The reason for this is likely connected with the earlier established fact that the mechanical properties of multilayer materials are determined by a number of ionic cross-links in the system, but practically independent of the stiffness of the building blocks. Clearly, our nanoparticles are incorporated inside the dendrimer, and do not have a contact with the alternating polyelectrolyte. In other words, their encapsulation inside dendrimers cannot affect the number of ionic cross-links. Note, however, that the fact that Au-loaded dendrimers are getting stiffer likely still plays some, but indirect role. One can speculate that the small increase in the slope of the force curves after encapsulation of gold (Fig. 5) is indeed due to the slight increase in the thickness of the dendrimer layer due to inner nanoparticles, which are expected to lead to a weaker "spreading" and compression of dendrimers on a template for a capsule preparation. From the analysis of the force curves one can also conclude that additional protective PSS layer increases the stiffness of the microcapsules due to an increase in the shell thickness, but presumably also due to the decrease in permeability. Thus, the experimental data suggest that the incorporated nanoparticles do not really increase the stiffness of the capsule shells, and the main parameter that controls the mechanical properties of the capsule shells is still the amount of ionic cross-links between alternating polyelectrolytes and dendrimers.

4. Conclusions

We have presented a novel method of assembling microshells loaded with gold nanoparticles and measured their mechanical properties. These microshells represent very promising and multifunctional systems, since, on one hand, they can be used as dual encapsulation and release systems; on the other hand, they consist of dendrimers which are also important for the variety of applications [48]; finally, they contain gold nanoparticles that impart other promising properties (optical, electrical, remote release and more). Remarkably, the use of nanoparticles encapsulated into dendrimers practically does not affect mechanical characteristics of the microshells.

Acknowledgements

We acknowledge the support of the Russian Foundation for Basic Research (Grant No. 07-03-00927). We thank G. Glasser for taking SEM images, K. Kirchhoff for taking TEM images and K. Klein for the Au-PAMAM solutions' preparation.

References

[1] Sukhorukov GB, Donath E, Lichtenfeld H, Knippel E, Knippel M, Budde A, et al. Colloids Surf A 1998;137(1–3):253–66.
[2] Vinogradova OI, Andrienko D, Lulevich VV, Nordschild S, Sukhorukov GB. Macromolecules 2004;37(3):1113–7.
[3] Stukan MR, Lobaskin V, Holm C, Vinogradova OI. Phys Rev E 2006; 73(2):021801.
[4] Tsekov R, Vinogradova OI. J Chem Phys 2007;126(9):094901.
[5] Vinogradova OI. J Phys Condens Matter 2004;16:R1105–34.
[6] Lulevich VV, Radtchenko IL, Sukhorukov GB, Vinogradova OI. J Phys Chem B 2003;107(12):2735–40.
[7] Kim BS, Fan TH, Lebedeva OV, Vinogradova OI. Macromolecules 2005; 38(19):8066–70.
[8] Vinogradova OI, Lebedeva OV, Kim BS. Annu Rev Mater Res 2006;36: 145–80.
[9] Shchukin DG, Sukhorukov GB, Möhwald H. Angew Chem Int Ed 2003; 42(37):4472–5.
[10] Shchukin DG, Ustinovich EA, Sukhorukov GB, Möhwald H, Sviridov DV. Adv Mater 2005;17(4):468–72.
[11] Lee D, Rubner MF, Cohen RE. Chem Mater 2005;17(5):1099–105.
[12] Zhao M, Sun L, Crooks RM. J Am Chem Soc 1998;120(19):4877–8.
[13] Balogh L, Tomalia DA. J Am Chem Soc 1998;120(29):7355–6.
[14] Esumi K, Suzuki A, Aihara N, Usui K, Torigoe K. Langmuir 1998; 14(12):3157–9.
[15] Esumi K, Hosoya T, Suzuki A, Torigoe K. Langmuir 2000;16(6):2978–80.
[16] Zhao MQ, Crooks RM. Angew Chem Int Ed 1999;38(3):364–6.
[17] Zhao M, Crooks RM. Adv Mater 1999;11(3):217–20.
[18] Gröhn F, Bauer BJ, Akpalu AY, Jackson CL, Amis EJ. Macromolecules 2000;33(16):6042–50.
[19] Gröhn F, Kim G, Bauer BJ, Amis EJ. Macromolecules 2001;34(7): 2179–85.
[20] Daniel MC, Astruc D. Chem Rev 2004;104(1):293–346.
[21] Krasteva N, Krustev R, Yasuda A, Vossmeyer T. Langmuir 2003;19(19): 7754–60.
[22] Zhao MQ, Crooks RM. Chem Mater 1999;11(11):3379–85.
[23] Niu YH, Crooks RM. C R Chim 2003;6(8–10):1049–59.
[24] Crooks RM, Zhao MQ, Sun L, Chechik V, Yeung LK. Acc Chem Res 2001;34(3):181–90.
[25] Bielinska A, Eichman JD, Lee I, Baker JR, Balogh L. J Nanopart Res 2002;4(5):395–403.
[26] Evenson SA, Badyal JPS. Adv Mater 1997;9(14):1097–9.

[27] He J-A, Valluzzi R, Yang K, Dolukhanyan T, Sung C, Kumar J, et al. Chem Mater 1999;11(11):3268–74.
[28] Esumi K, Akiyama S, Yoshimura T. Langmuir 2003;19(18):7679–81.
[29] Fendler JH, editor. Nanoparticles and nanostructured films. Preparation, characterization and applications. Weinheim, Germany: Wiley-VCH; 1998.
[30] Dubreuil F, Shchukin DG, Sukhorukov GB, Fery A. Macromol Rapid Commun 2004;25(11):1078–81.
[31] Jiang C, Markutsya S, Tsukruk VV. Adv Mater 2004;16(2):157–61.
[32] Jiang C, Markutsya S, Pikus Y, Tsukruk VV. Nat Mater 2004;3(10):721–8.
[33] Khopade A, Caruso F. Biomacromolecules 2002;3(6):1154–62.
[34] Khopade A, Caruso F. Nano Lett 2002;2(8):415–8.
[35] Kim BS, Lebedeva OV, Kim DH, Caminade AM, Majoral JP, Knoll W, et al. Langmuir 2005;21(16):7200–6.
[36] Kim BS, Lebedeva OV, Koynov K, Gong H, Caminade AM, Majoral JP, et al. Macromolecules 2006;39(16):5479–83.
[37] Certain commercial materials and equipments are identified in this article in order to specify adequately the experimental procedure. In no case does such identification imply recommendation by the National Institute of Standards and Technology, nor does it imply that the material or equipment identified is necessarily the best available for this purpose.
[38] Jackson CL, Chanzy HD, Booy FP, Drake BJ, Tomalia DA, Bauer BJ, et al. Macromolecules 1998;31(18):6259–65.
[39] Lulevich VV, Nordschild S, Vinogradova OI. Macromolecules 2004; 37(20):7736–41.
[40] Lulevich VV, Radtchenko IL, Sukhorukov GB, Vinogradova OI. Macromolecules 2003;36(8):2832–7.
[41] Lulevich VV, Andrienko D, Vinogradova OI. J Chem Phys 2004;120(8): 3822–6.
[42] Lulevich VV, Vinogradova OI. Langmuir 2004;20(7):2874–8.
[43] Sader JE, Larson I, Mulvaney P, White LR. Rev Sci Instrum 1995;66(7): 3789–98.
[44] Cleveland JP, Manne S, Bocek D, Hansma PK. Rev Sci Instrum 1993; 64(2):403–5.
[45] Lebedeva OV, Kim BS, Vasilev K, Vinogradova OI. J Colloid Interface Sci 2005;284(2):455–62.
[46] Kohler K, Shchukin D, Mohwald H, Sukhorukov G. J Phys Chem B 2005;109(39):18250–9.
[47] Bliznyuk VN, Rinderspacher F, Tsukruk VV. Polymer 1998;39(21): 5249–52.
[48] Frechet JMJ, Tomalia DA, editors. Dendrimer and other dendritic polymers. Chichester; 2001.